Journal of Scientific and Technical Research
15 (1) 2025, 01-08
www.publishingindia.com/jstr

Comprehensive Review on Adsorption Behaviors of Bromine

Shivani Varshney[1], Shalu[2] and Babita Tripathi[2*]
[1]Micron Technology, Inc., Boise, Idaho, USA
[2]Department of Engineering & Sciences, Sharda University, Greater Noida, Uttar Pradesh, India
[*]Corresponding Author: babita.tripathi@sharda.ac.in

Abstract: Phases and thin films have been an interesting topic in the world of materials science. Adsorption of an adatom on a substrate result in exceptional properties than the bulk phase, its deposition often performed in ultra-high vacuum. These extraordinary physical, chemical and electronic properties find applications in solar cells, sensors, metal interconnects of circuits, protective coatings and spintronic devices. Halogens have been widely studied for their metal etching reactions. This study provides a review of bromine adsorption on different substrates. The adsorption has resulted in many phases and reconstructions, studied using scanning tunnelling microscopy, low energy electron diffraction and density functional theory. Understanding the formation and dissociation of bromine phases provides a crucial insight about how bromine behaves at atomic levels and can result in improvement in the power conversion efficiency and junction quality of solar cells and metal interconnects.

Keywords: Adsorption, Bromine, Density functional theory, Deposition, Low energy electron diffraction, Nanostructures, Perovskites, Phases, Scanning tunnelling microscopy, Thin films.

I. Introduction

Halogens have been widely investigated for their physical and chemical interactions on metal surfaces. Halogen etching has played an important role in the fabrication of interconnects in the electronic devices [1, 2]. It has been known that halogens like chlorine (Cl), iodine (I) and bromine (Br) are strongly adsorbed on metal surfaces like platinum (Pt), gold (Au), silver (Ag), and copper (Cu), therefore, play a significant part in electrochemical reactions [3-9]. To understand fundamental concepts of adsorption of these halogens, many studies have also been published on silicon (Si) and gallium arsenide (GaAs) surfaces [10]. These low-dimension systems have the capability to switch between different phases based on their microscopic interactions with the substrate [11-13]. This review article focusses on adsorption of thin films of bromine on Pt(110), Cu(100), Ni(110) and Ge(001). A report on Br adsorption on Pt(110) shows the formation of *c*(2x2) phase at Br coverage of 0.5 monolayer (ML) [9]. At a coverage of 0.58 ML, another phase has been observed and identified as (3x1) phase [9]. Both these phases have been verified by low energy electron diffraction (LEED) and scanning tunneling microscopy (STM) images. The paper examines the phase transition from the *c*(2x2) to the (3x1) phase [9]. Their DFT results show relatively higher energy for (3x1) phase indicating a less favourable state, however their experimental results indicate the phase transition could be due to a charge density wave (CDW) phase [9]. Studies have been performed by Altnam *et al.,* stating that at low coverages, it is difficult to image Br or Cl on Cu(100). This could be due to the tip induced motion of halogen atoms inhibiting motion of adsorbate atoms [14-16]. A halogen overlayer with *c*(2x2) halogen reconstruction has been reported along with CuCl and CuBr at high coverages on Cu(100) [14-16]. In one of the reports, authors have studied the molecular Br interaction on Ni(110) [17]. This study has been performed using scanning tunneling microscopy at room temperature. At low coverages, Br forms a basic structure where two pairs of Br atoms are aligned parallel to each other [17]. At higher coverages, it forms *p*(3x2) reconstruction upon annealing [17]. Some other studies of halogen deposition have been performed on Si(001) and Ge(001) substrates [18]. It has been found that the halide molecules dissociate into atoms and get adsorbed on the substrate without breaking the substrate's dimer bond [18]. At 0.5 ML of iodine, Si(001) forms *c*(2x2) reconstruction and at 1 ML of iodine, it forms *p*(2x1) reconstruction [19]. On Ge(001) substrate, the initial reconstruction was *p*(1x2), it changes to mixed *p*(2×2)/*c*(2×4) upon adsorption of iodine [20]. In another report, authors have investigated all different configurations of Br upto 1 ML deposited on *p*(1x2) reconstructed Ge (001) surface [18]. The paper by J. Inukai reports deposition of bromine on Cu(100) which results in the *c*(p×√3R-30°) structure [21]. This result has been verified using STM and LEED [21].

II. Experimental Details

A. Br/Pt (110) Deposition

The experiments were performed in UHV (ultra high vacuum) STM with the base pressure less than $8x10^{-11}$ mbar [22]. Br was deposited from a solid-state electrolysis cell. Two phases were

observed. At 0.5 ML coverage, *c*(2x2) phase was obtained [23]. At 0.58 ML coverage, (3x1) phase was formed [9]. These phases have been confirmed by STM images, LEED and DFT calculations (density functional theory). STM images have been taken at constant current mode and the bias voltage in all the figures refer to sample bias [9]. A charge-coupled device camera was used to record LEED images using AIDA-PC [24]. (I)E spectra and special spot profile were recorded. I(E) spectra was recorded at 130 K and in steps of 0.5 eV from 40 to 400 eV [9, 10]. Spot profiles were taken at 370 K in order to achieve both c(2x3) phase and (3x1) phase. Fig. 1 shows the STM images and corresponding LEED patterns for 0.5 ML and 0.58 ML Br coverage on Pt(110) [10].

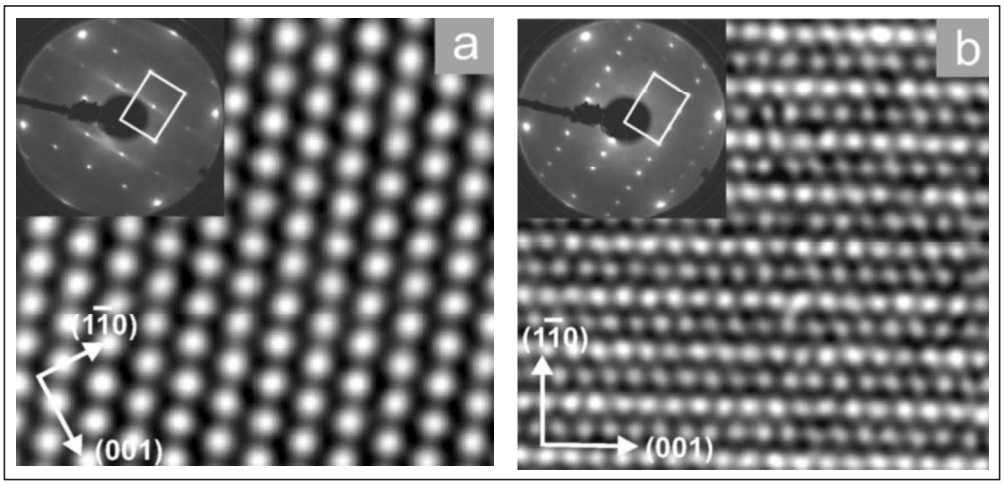

Fig. 1: (a) An STM Image of 50x50 $Å^2$ Taken at (~0.82 V, 1.14 nA) Along with a LEED Pattern (E=147 eV) of the *c*(2x2) Phase with a Br Coverage of 0.5 ML (b) An STM Image of 70x70 $Å^2$ Taken at (~12 mV, 0.63 nA) and LEED Pattern (E=147 eV) of a (3x1) Phase with a Br Coverage of 0.58 ML [9]

For first-principles DFT calculations, two methods were used. The first one is all-electron full potential linearized augmented plane-wave (FLAPW) Method [25] and the Vienna ab initio simulation Package ~VASP [26]. A detailed description of these calculation has been reported in the study performed by C. Deisl *et al*. [9].

B. Br/Ni (110) Deposition

Ni (110) substrate was mechanically polished and ultrasonically rinsed in double distilled water [17]. All experiments were performed in commercial Omicron UHV-STM at room temperature [17]. Tungsten tips were used in experiments. For the pressure, ion and turbo pumps were used to create a pressure of $4x10^{-11}$ mbar [17]. XPS (X-ray Photoelectron Spectroscopy) and LEED have been attached to the UHV chambers. Ni substrate was cleaned using Ar ions repeated cycles at 1.4 kV ad 10 μA for 30 minutes [17]. The sample was annealed at 700 °C for 20 minutes. It was made sure that LEED indicate (1x1) surface and it is free of any impurities verified by XPS and STM imaging [17]. For Br sources, an electrochemical Ag/AgBr–$CdBr_2$/Pt cell was used. Before deposition, the sources were outgassed so that oxygen or hydrogen bromide was not present in the incident Br beam [27].

C. Br/Ge (001) Deposition

For STM imaging, a tungsten tip formed by 5-atom pyramid with (001) orientation has been used [18]. For the interactions between the tip and the substrate calculations based on Fireball approach has been utilized [28]. The STM images were simulated in constant-height mode. The sample bias was -1eV and tip-sample distance was 8 Å [18]. For DFT calculations two methods have been deployed. A plane-wave-basis (pw) technique and a local-orbital minimal-basis (lo) technique [29, 30]. For local orbital technique, the Fireball2007 code has been used [31, 32]. For Fireball calculations, VASP package has been utilized [33-36]. For ion cores, FHI98PP package [37] has been applied. Different schemes including Troullier and Martins [38] and Hamann [39] have been used for determining Ge and Br pseudopotential. Exchange-correlations with local-density approximation were used [40-42].

D. Br/Cu (111) Deposition

Single crystal Cu(111) substrate with 5 mm diameter was used for Br deposition [21]. Acetone, methanol, and pure water were used to clean and sonicate the substrate [21]. The surface was further cleaned by phosphoric and sulphuric acid [21]. KBr solution was used to study Br structures. For STM imaging, tungsten tip was used. In order to reduce residual currents, the tip was polished [43]. Analysis, preparation and electrochemical chambers were present in the UHV system. It also consisted of *in-situ* LEED as reported in various studies [43-46]. KBr solution was prepared from KANTO CHEMICAL (Cica-Reagent grade), and ultrapure water (Millipore-Q). The reference electrode was a saturated calomel electrode (SCE) [21].

III. Results and Discussion

A. Br/Pt (110) Structure

Deposition of Br on pt(110) has been studied by the authors using STM [13]. At 1/2 ML coverage, Br forms *c*(2x2) phase where every second short bridge site has been occupied by Br atoms on Pt(110) surface [9]. An image of this *c*(2x2) phase [9] has been shown by Fig. 1 (a). At a coverage of 2/3 ML(~0.6 ML), Br transits from *c*(2x2) phase to (3x1) phase where Br is present on every third short-bridge and long-bridge sites [9] as shown by an STM image in Fig. 1 (b).

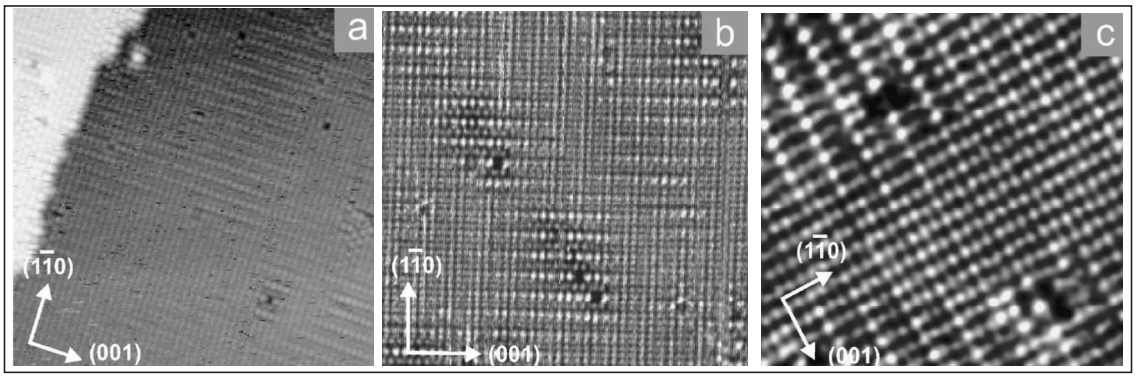

Fig. 2: (a) An STM Image of Br Coverage of 0.51 ML Where *c*(2x2) Phase is Seen at the Steps and (3x1) Phase on Terraces Surrounded by (1x1) Phase (b) At 0.54 ML Coverage, Three (3x1) Antiphase have been Shown (c) 0.54 ML Coverage Prepared by Desorption from Higher Coverage, (3x1) Phase with the Continuous Change in Modulation Strength has been Shown. The Images have been taken from the Reference [9]

At a coverage between 1/2 ML and 0.58 ML, STM images show the nucleation of (3x1) islands along with 1/2 ML coverage areas. With Br addition of 0.01 ML to 1/2 ML (total 0.51 ML), ***c***(2x2) phase is mostly seen at the steps or around the defects [9]. On the terraces, (3x1) phase surrounded by (1x1) disordered areas [9] can be seen in Fig. 2 (a). At 0.54 ML coverage of Br, their (3x1) antiphase domains can be observed by Fig. 2 (b). If 0.54 ML of Br is prepared by thermal desorption from a higher coverage, again a (3x1) phase can be seen with the continuous change in modulation strength. Fig. 2 (c) shows an STM image for this case [9].

B. Br/Ni (110) Structure

i) Low Br Coverage

Fig. 3 (a) shows an STM image of Ni(110) surface where the surface forms close packed rows with an atomic spacing of a/√2, a=3.52 Å. Fig. 3 (b) indicates defects in the form of Ni vacancies [17].

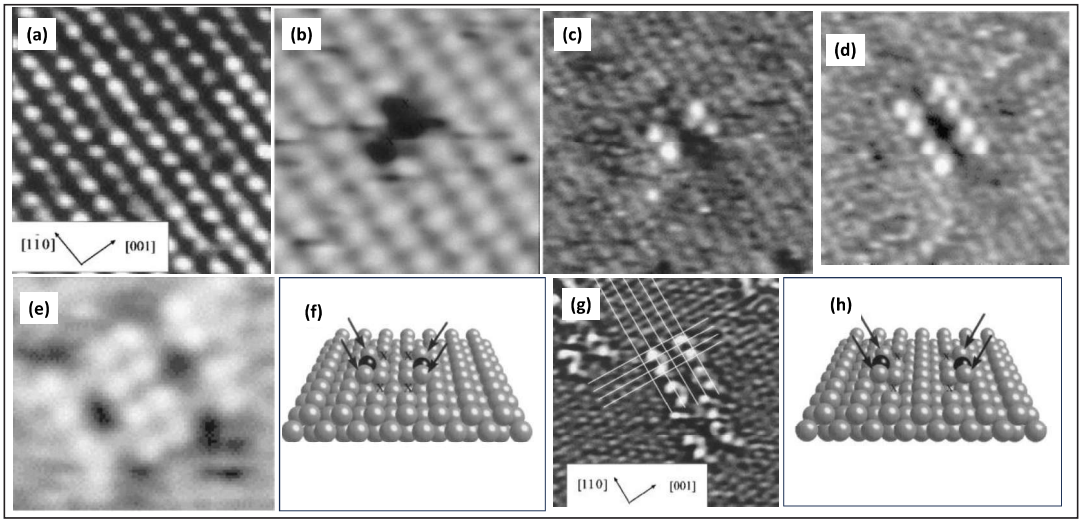

Fig. 3: (a) Clean Ni(110) Surface at a Tunnel Current of 5 nA, and sample bias −0.14 V (b) Defects on Ni Clean Surface Scanned at Tunnel Current of 4 nA, Sample Bias of −0.01 V (c) Image Showing a Butterfly Feature at Tunnel Current of 1 nA, and Sample Bias of −0.01 V (d) Aggregation of the Units After Annealing at 100 °C in [1$\bar{1}$0] Direction (e) Aggregation of the Units in [001] Direction, Both at Tunnel Current of 1 nA and Sample Bias of −0.01 V (g) Four Butterfly Features in [1$\bar{1}$0] and [001] Direction with Tunnel Current 5 nA, Sample Bias −0.01 V (h) Model for Structure Shown in (g), Where Dark Spheres are Br, Light Spheres are Ni [17]

At a Br coverage of 2.3 x 10^{13} Br atoms/cm^2, Ni(110) surface marks the formation of two discrete pairs of maxima as shown in Fig. 3 (c) [17]. The shape has been referred as "butterfly" shape. The authors have presented a model where the greyscale maxima correspond to Ni adatoms in two-fold hollow sites adjacent to a dissociated Br atom [17]. Each pair is bound with a single Br atom. The corresponding model has been shown in Fig. 3 (f). Annealing of the surface at 100 °C for 10 minutes results in aggregation of butterflies as shown in Fig. 3 (d). It also forms adsorption islands of between two and eight units as shown in Fig. 3 (e). The mechanism explored by the authors contains the diffusion of $BrNi_2$ units along $[1\bar{1}0]$ direction in the troughs between the close packed rows. Fig. 3 (g) supports the diffusion theory of $BrNi_2$ where butterfly aggregation has taken place. The corresponding model has been shown in Fig. 3 (h). Each figure has been obtained from reference [17].

ii) High Br Coverage

At a higher coverage of 0.51 x 10^{15} Br atoms/cm^2, $BrNi_2$ units have formed clusters as shown by Fig. 4 (a). Annealing at 200 °C for 20 minutes result in surface reconstruction as shown by Fig. 4 (b). Fig. 4 (c) shows a high resolution image of the surface reconstruction and has been identified as *p*(3 x 2) reconstruction [49]. At this point, Br coverage is 0.6×10^{15} Br atoms/cm^2. LEED pattern shown in Fig. 4 (d) aligns with (3 x 2) pattern on Ni(110). Authors have provided a model [17] for this superstructure as shown in Fig. 4 (e). It involves alternating atomic sequences of Ni-Br-Br-Ni-Br-Br-Ni and Br-Ni-Ni-Br-Ni-Ni-Br. All these images have been obtained from reference [17].

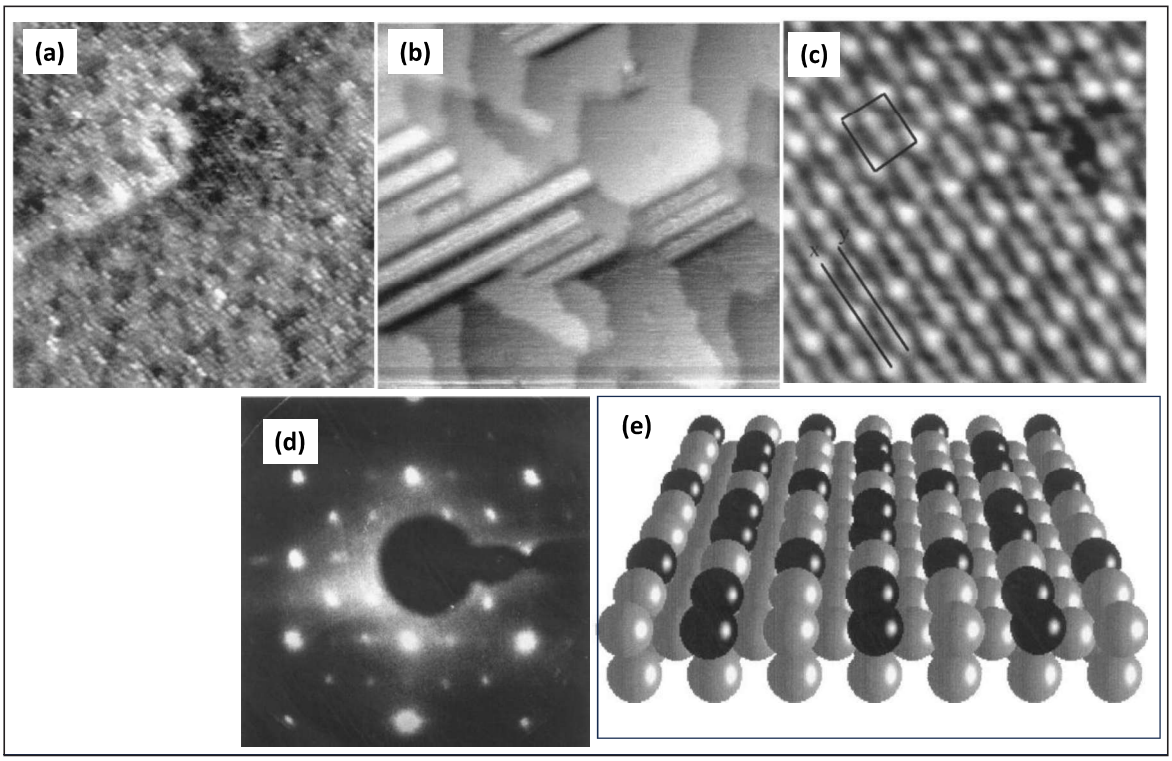

Fig. 4: (a) High Br Coverage on Ni Surface (b) Annealing at 200°C for 30 min. (c) The (3×2) Cell is Highlighted. All the Three Images have been Taken at at Tunnel Current of 3 nA, Sample Bias of −0.01 V (d) LEED Pattern for (3x2) Surface Reconstruction Taken at 70 eV (e) Model Presented for Br Reconstruction, Where Dark Spheres are Br, Light Spheres are Ni. The Images have been Taken from the Reference [17]

iii) Br/Ge (001) Structure

0.25 ML of Br has been deposited on *p*(1x2) reconstructed Ge (001) substrate [18]. Four stable configurations have been observed, i.e., hexagonal, *p*(1 ×4), *p*(2 ×2) and *p*(2 ×4) [18].

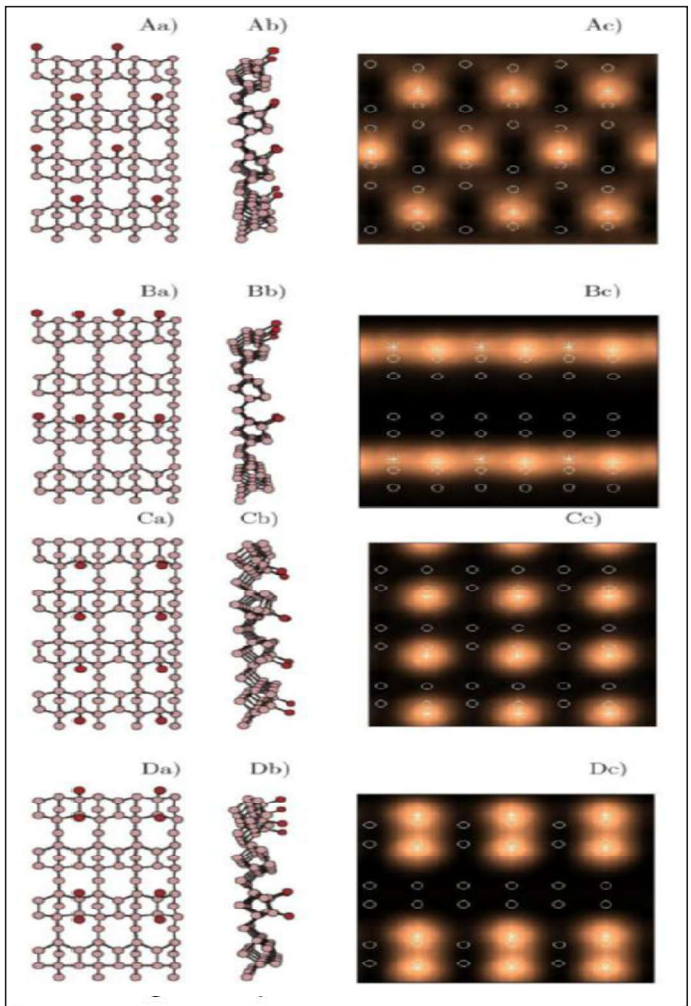

Structure	hex, A		p(1×4), B		p(2×2), C		p(2×4), D	
Method	lo	pw	lo	pw	lo	pw	lo	pw
Energy [eV]	0.46	0.18	0.52	0.21	0.33	0.12	0	0
Avg. b. l. [Å]	2.24	2.34	2.36	2.33	2.36	2.34	2.36	2.33
E_{ads} [eV]	-3.10	-3.3	-3.04	-3.32	-3.23	-3.41	-3.56	-3.53
Avg. ht. [Å]	1.27	1.78	1.79	2.05	1.94	2.03	2.06	2.01

Fig. 5: For 0.25 ML Br on Ge (001), Four Atomic Models and Reconstructions have been Shown. A) Shows Hexagonal, B) p(1×4), C) p(2×2), and D) p(2×4) Reconstructions. (a) is the Top View and (b) is the Side View of Each Surface Configuration with Darker and Brighter Balls Denoting Br and Ge Atoms, Respectively (c) are the Simulated STM Images with Br Adatoms and Ge Surface Dimer Atoms are Marked by Stars and Circles, Respectively. Bias Voltage is -0.1 V. Table I Shows Data Associated with These Reconstructions [18]

All these four reconstructions with models and simulated images have been shown in Fig. 5. The adsorbate atoms interacted with Ge through dangling bonds in all the first three structures. However, in *p*(2x4) reconstruction, Br atoms interacted with the both sides of the same Ge dimer, which resulted in the most energetically favoured reconstruction [18]. This case is similar to studies presented for other halides adsorption on Ge and Si substrates [10, 19, 47]. Table I sums up different methods of calculations, minimum energy configurations, average Ge-Br bond length, adsorption energy per molecule and average height of Br adatoms and Ge atoms [18].

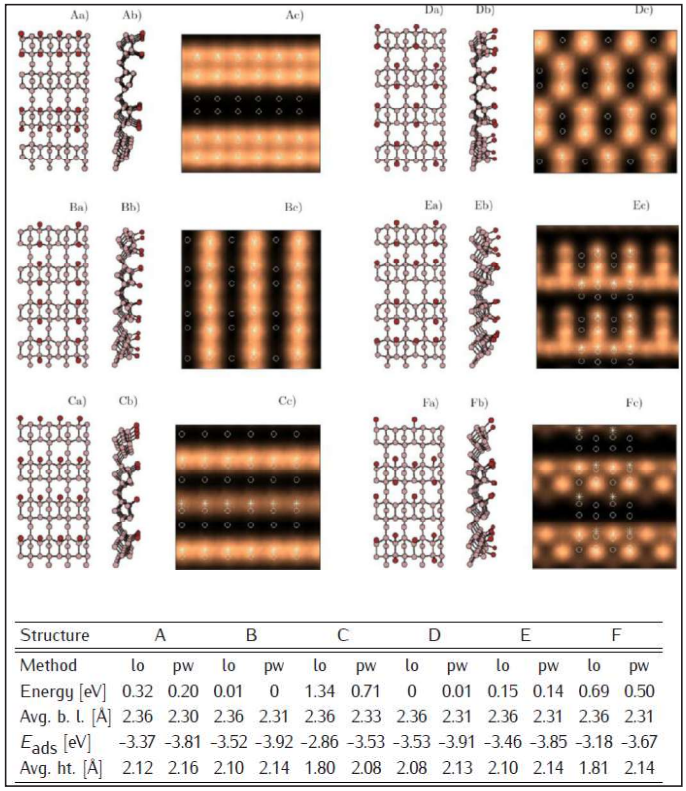

Structure	A		B		C		D		E		F	
Method	lo	pw	lo	pw	lo	pw	lo	pw	lo	pw	lo	pw
Energy [eV]	0.32	0.20	0.01	0	1.34	0.71	0	0.01	0.15	0.14	0.69	0.50
Avg. b. l. [Å]	2.36	2.30	2.36	2.31	2.36	2.33	2.36	2.31	2.36	2.31	2.36	2.31
E_{ads} [eV]	-3.37	-3.81	-3.52	-3.92	-2.86	-3.53	-3.53	-3.91	-3.46	-3.85	-3.18	-3.67
Avg. ht. [Å]	2.12	2.16	2.10	2.14	1.80	2.08	2.08	2.13	2.10	2.14	1.81	2.14

Fig. 6: For 0.5 ML Br on Ge (001), Six Atomic Models and Reconstructions have been Shown (b) Is the Side View of Each Surface Configuration with Darker and Brighter Balls Denoting Br and Ge Atoms, Respectively (c) Are the Simulated STM Images with Br Adatoms and Ge Surface Dimer Atoms are Marked by Stars and Circles, Respectively. Bias Voltage is -0.1 V. Table II Shows Data Associated with These Reconstructions. The Images have been Taken from the Reference [18]

At 0.5 ML of Br, six reconstructions in a *p*(2×4) surface cell have been observed. These reconstructions have been shown in Fig. 6 along with Table II. As previously stated by the authors, two energetically favorable configurations were those where adatoms were bound to both ends of the same Ge(001) dimers. At 0.75 ML of Br, two stable reconstructions were observed. At 1 ML, one reconstruction was found [18]. Fig. 7 along with Table III explains these configurations and data associated with them.

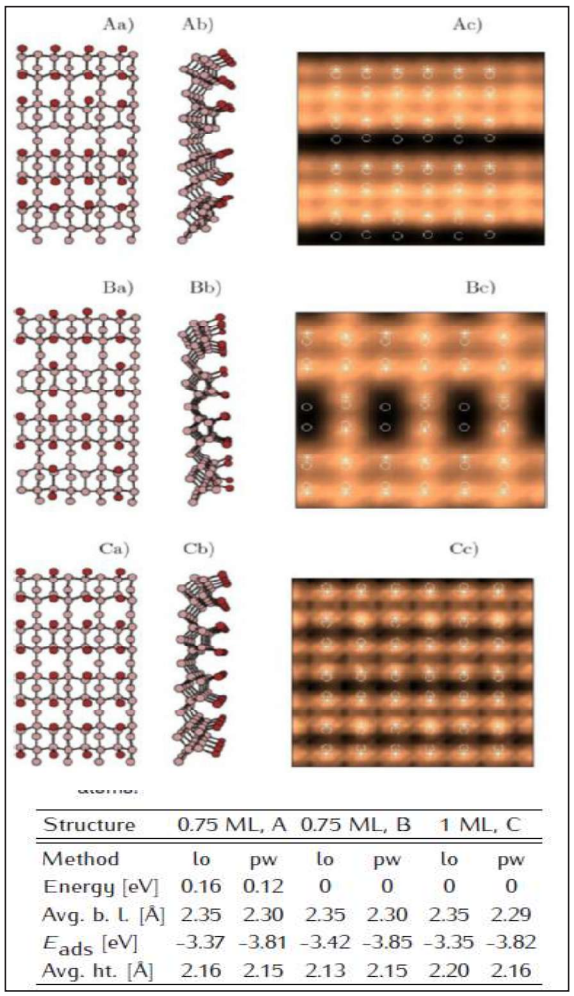

Structure	0.75 ML, A		0.75 ML, B		1 ML, C	
Method	lo	pw	lo	pw	lo	pw
Energy [eV]	0.16	0.12	0	0	0	0
Avg. b. l. [Å]	2.35	2.30	2.35	2.30	2.35	2.29
E_{ads} [eV]	-3.37	-3.81	-3.42	-3.85	-3.35	-3.82
Avg. ht. [Å]	2.16	2.15	2.13	2.15	2.20	2.16

Fig. 7: A) and B) For 0.75 ML and C) for 1ML Br on Ge (001), a) Two Atomic Models and Reconstructions have been Shown (b) Is the Side View of Each Surface Configuration with Darker and Brighter Balls Denoting Br and Ge Atoms, Respectively (c) Are the Simulated STM Images with Br Adatoms and Ge Surface Dimer Atoms are Marked by Stars and Circles, Respectively. Bias Voltage is -0.1 V. Table III Shows Data Associated with These Reconstructions [18].

iv) Br/Cu(111) Structure

Before Br deposition on Cu(111) substrate, bare Cu(111) has been imaged by *in-situ* STM in 0.1 M $HClO_4$ at -0.6 V [21]. The authors found the terraces to be atomically flat. Their high-resolution image shows that Cu (111) has hexagonal lattice with a lattice constant of 0.256 nm and an angle of 60° between the atomic rows [21]. LEED pattern for Br is similar to that of Cl [48-50]. At low coverage, Br forms (√3 x√3)R30° structure. At high coverages it get changed to (9√3 x9√3)R30° [50].

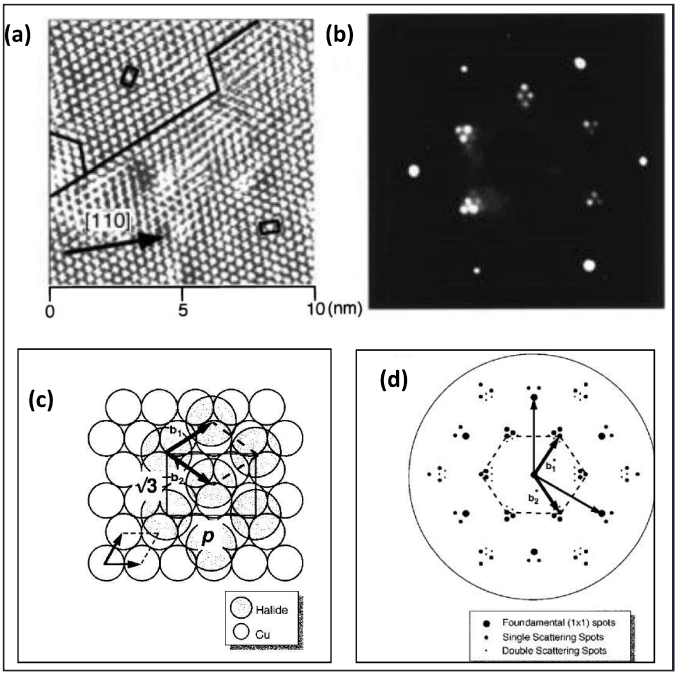

Fig. 8: (a) An STM Image of Br Adlayer on Cu(111) at -0.05 V and 5 nA Tunneling Current, in 0.01 M $HClO_4$ + 0.1 mM KBr. Tunneling Current was 5 nA. (b) Corresponding LEED Pattern (c) c(*p* x3*R*-30°) Lattice on Cu(111) (d) Calculated LEED Pattern for (c). The Images have been Taken from the Reference [21]

Based on STM images, it has not corresponded to (√3 x√3)*R*30° structure as the longer side of the rectangular unit cell is shorter than 3 times the Cu-Cu distance [21]. The domain boundaries and rectangular cell has been shown in Fig. 8 (a). The *p* value measured on STM image is ~2.6 [21]. Corresponding LEED pattern has been shown in Fig. 8 (b) and it looks similar to c(*p* x√3*R*-30°) structure [21]. The *p* value aligns with the STM image [21]. A model and corresponding LEED pattern has been shown in Fig. 8 (c) and (d).

IV. Conclusion

Many studies have been reported on Br deposition and formation of different phases on various substrates. In this paper, we have reviewed Br deposition on Pt (110), Ni (110), Ge (001) and Cu (111). Br deposition on Pt(110) resulted in transition of *c*(2x2) phase to (3x1) phase. Br on Ni (110) study showed the formation of a butterfly structure at low coverage and formation of (3x2) reconstruction on higher coverage. Deposition of Br on Ge (001) was performed at 0.25 ML, 0.5 ML, 0.75 ML and 1 ML resulted in many reconstruction configurations. It was found that Br adsorption on both ends of

the same Ge dimer has lowest energy system and hence most favorable configuration. Cu(111) study reveals that at low coverage, Br forms ($\sqrt{3}$ x$\sqrt{3}$)*R*30° structure. At high coverages it gets changed to (9$\sqrt{3}$ x9$\sqrt{3}$)*R*30°**.** Understanding of these Br phases would aid in making reliable and stable interconnects in electronic devices. Also, Br based inorganic perovskites find massive applications in solar cells. Understanding of these phases can assist in Br interaction within these solar cells for higher efficiency.

Declaration of Competing Interest

There are no competing interests to influence the work reported in this paper.

References

[1] J. Intrater, *Materials and Manufacturing Processes*, vol. 8, p. 743, 1993, doi: https://doi.org/10.1080/10426919308934878.

[2] S. Wolf, and R. N. Tauber, *Silicon Processing for the VLSI Era.* 2000. [Online]. Available: doi: https://books.google.com/books?id=fAuKQgAACAAJ

[3] A. T. Hubbard, *Chemical Reviews*, vol. 88, p. 633, 1988, doi: https://doi.org/10.1021/cr00086a004.

[4] F. Lu, G. N. Salaita, H. Baltruschat, and A. T. Hubbard, *Journal of Electroanalytical Chemistry and Interfacial Electrochemistry*, vol. 222, p. 305, 1987. [Online]. Available: https://www.sciencedirect.com/science/article/pii/0022072887802954

[5] B. G. Bravo, S. L. Michelhaugh, M. P. Soriaga, I. Villegas, D. W. Suggs, and J. L. Stickney, *The Journal of Physical Chemistry*, vol. 95, p. 5245, 1991, doi: https://doi.org/10.1021/j100166a060.

[6] G. N. Salaita, F. Lu, L. Laguren-Davidson, and A. T. Hubbard, *Journal of Electroanalytical Chemistry and Interfacial Electrochemistry*, vol. 229, no. 1, 1987, doi: https://doi.org/10.1016/0022-0728(87)85127-6.

[7] M. E. Bothwell, G. J. Cali, G. M. Berry, and M. P. Soriaga, *Surface Science Letters*, vol. 249, p. L322, 1991. [Online]. Available: https://www.sciencedirect.com/science/article/pii/0167258491901147

[8] M. Hourani, M. Wasberg, C. Rhee, and A. Wieckowski, *Croatica Chemica Acta*, vol. 63, p. 373, 1990. [Online]. Available: https://hrcak.srce.hr/137379

[9] C. Deisl, K. Swamy, N. Memmel, E. Bertel, C. Franchini, G. Schneider, . . . K. Heinz, *Physical Review B*, vol. 69, p. 195405, 2004, doi: https://link.aps.org/doi/10.1103/PhysRevB.69.195405

[10] D. Rioux, F. Stepniak, R. J. Pechman, and J. H. Weaver, *Physical Review B*, vol. 51, p. 10981, 1995, doi: https://link.aps.org/doi/10.1103/PhysRevB.51.10981.

[11] A. R. Bishop, *Synthetic Metals*, vol. 86, p. 2203, 1997. [Online]. Available: https://www.sciencedirect.com/science/article/pii/S037967799781096X

[12] S. Sachdev, *Science*, vol. 288, p. 475, 2000, doi: https://doi.org/10.1126/science.288.5465.475.

[13] C. Deisl, K. Swamy, R. Beer, A. Menzel, and E. Bertel, *Journal of Physics: Condensed Matter,* vol. 14, p. 4199, 2002, doi: https://dx.doi.org/10.1088/0953-8984/14/16/311.

[14] C. Y. Nakakura, and E. I. Altman, *Journal of Vacuum Science & Technology A,* vol. 16, p. 1566, 1998, doi: https://doi.org/10.1116/1.581188.

[15] C. Y. Nakakura, and E. I. Altman, *Surface Science*, vol. 370, p. 32, 1997. [Online]. Available: https://www.sciencedirect.com/science/article/pii/S0039602896009508

[16] C. Y. Nakakura, V. M. Phanse, and E. I. Altman, *Surface Science,* vol. 370, p. L149, 1997. [Online]. Available: https://www.sciencedirect.com/science/article/pii/S0039602896011715

[17] T. W. Fishlock, J. B. Pethica, A. Oral, R. G. Egdell, and F. H. Jones, *Surface Science*, 426, p. 212, 1999. [Online]. Available: https://www.sciencedirect.com/science/article/pii/S0039602899003234

[18] P. MikoÅ‚ajczyk, and B. Stankiewicz, vol. 7, p. 279, 2009, doi: https://doi.org/10.2478/s11534-008-0142-x.

[19] G. A. de Wijs, A. De Vita, and A. Selloni, *Physical Review B*, vol. 57, p. 10021, 1998, doi: https://link.aps.org/doi/10.1103/PhysRevB.57.10021.

[20] M. Göthelid, G. Le Lay, and U. O. Karlsson, *Surface Science*, vol. 556, p. 203, 2004. [Online]. Available: https://www.sciencedirect.com/science/article/pii/S0039602804002699

[21] J. Inukai, Y. Osawa, and K. Itaya, *The Journal of Physical Chemistry B*, vol. 102, p. 10034, 1998, doi: https://doi.org/10.1021/jp982952l.

[22] L. Alting, F. Kimura, H. N. Hansen, and G. Bissacco, *CIRP Annals,* vol. 52, p. 635, 2003. [Online]. Available: https://www.sciencedirect.com/science/article/pii/S000785060760208X

[23] V. Blum, L. Hammer, K. Heinz, C. Franchini, J. Redinger, K. Swamy, . . . E. Bertel, *Physical Review B*, vol. 65, p. 165408, 2002, doi: https://link.aps.org/doi/10.1103/PhysRevB.65.165408.

[24] K. Heinz, *Reports on Progress in Physics*, vol. 58, p. 637, 1995, doi: https://dx.doi.org/10.1088/0034-4885/58/6/003.

[25] M. Weinert, E. Wimmer, and A. J. Freeman, *Physical Review B,* vol. 26, p. 4571, 1982, doi: https://link.aps.org/doi/10.1103/PhysRevB.26.4571.

[26] S. Wolf, and R. N. Tauber, 2000.

[27] G. Comelli, V. R. Dhanak, M. Kiskinova, G. Paolucci, K. C. Prince, and R. Rosei, *Surface Science*, vol. 269-270, p. 360, 1992. [Online]. Available: https://www.sciencedirect.com/science/article/pii/003960289291275G

[28] J. P. Perdew, and A. Zunger, *Physical Review B*, vol. 23, p. 5048, 1981, doi: https://link.aps.org/doi/10.1103/PhysRevB.23.5048.

[29] A. A. Demkov, J. Ortega, O. F. Sankey, and M. P. Grumbach, *Physical Review B*, vol. 52, p. 1618, 1995, doi: https://link.aps.org/doi/10.1103/PhysRevB.52.1618.

[30] O. F. Sankey, and D. J. Niklewski, *Physical Review B*, vol. 40, p. 3979, 1989, doi: https://link.aps.org/doi/10.1103/PhysRevB.40.3979.

[31] J. P. Lewis, K. R. Glaesemann, G. A. Voth, J. Fritsch, A. A. Demkov, J. Ortega, and O. F. Sankey, *Physical Review B*, vol. 64, p. 195103, 2001, doi: https://link.aps.org/doi/10.1103/PhysRevB.64.195103.

[32] P. Jelínek, H. Wang, J. P. Lewis, O. F. Sankey, and J. Ortega, *Physical Review B*, vol. 71, p. 235101, 2005, doi:https://link.aps.org/doi/10.1103/PhysRevB.71.235101.

[33] G. Kresse, and J. Hafner, *Physical Review B*, vol. 55, p. 7539, 1997, doi: https://link.aps.org/doi/10.1103/PhysRevB.55.7539.

[34] G. Kresse, and J. Furthmüller, *Computational Materials Science*, vol. 6, p. 15, 1996. [Online]. Available: https://www.sciencedirect.com/science/article/pii/0927025696000080

[35] G. Kresse, and J. Furthmüller, *Physical Review B*, vol. 54, p. 11169, 1996, doi: https://link.aps.org/doi/10.1103/PhysRevB.54.11169.

[36] G. Kresse, and D. Joubert, *Physical Review B*, vol. 59, p. 1758, 1999, doi: https://link.aps.org/doi/10.1103/PhysRevB.59.1758.

[37] M. Fuchs, and M. Scheffler, *Computer Physics Communications*, vol. 119, p. 67, 1999. [Online]. Available: https://www.sciencedirect.com/science/article/pii/S001046559800201X

[38] N. Troullier, and J. L. Martins, *Physical Review B*, vol. 43, p. 1993, 1991, doi: https://link.aps.org/doi/10.1103/PhysRevB.43.1993.

[39] D. R. Hamann, *Physical Review B*, vol. 40, p. 2980, 1989, doi: https://link.aps.org/doi/10.1103/PhysRevB.40.2980.

[40] J. P. Perdew, J. A. Chevary, S. H. Vosko, K. A. Jackson, M. R. Pederson, D. J. Singh, and C. Fiolhais, *Physical Review B*, vol. 46, p. 6671, 1992, doi: https://link.aps.org/doi/10.1103/PhysRevB.46.6671.

[41] X. Gonze, R. Stumpf, and M. Scheffler, *Physical Review B*, vol. 44, p. 8503, 1991, doi: https://link.aps.org/doi/10.1103/PhysRevB.44.8503.

[42] L. Kleinman, and D. M. Bylander, *Physical Review Letters*, vol. 48, p. 1425, 1982, doi: https://link.aps.org/doi/10.1103/PhysRevLett.48.1425.

[43] N. Batina, T. Yamada, and K. Itaya, *Langmuir*, vol. 11, p. 4568, 1995, doi: https://doi.org/10.1021/la00011a062.

[44] T. Yamada, N. Batina, and K. Itaya, *The Journal of Physical Chemistry*, vol. 99, p. 8817, 1995, doi: https://doi.org/10.1021/j100021a057.

[45] T. Yamada, N. Batina, and K. Itaya, *Surface Science*, vol. 335, p. 204, 1995. [Online]. Available: https://www.sciencedirect.com/science/article/pii/0039602895004173

[46] T. Yamada, K. Ogaki, S. Okubo, and K. Itaya, *Surface Science*, vol. 369, p. 321, 1996. [Online]. Available: https://www.sciencedirect.com/science/article/pii/S0039602896008801

[47] B. Stankiewicz, *Applied Surface Science*, vol. 254, p. 4380, 2008. [Online]. Available: https://www.sciencedirect.com/science/article/pii/S0169433208000731

[48] C. L. A. Lamont, H. Conrad, and A. M. Bradshaw, *Surface Science*, vol. 287-288, p. 169, 1993. [Online]. Available: https://www.sciencedirect.com/science/article/pii/003960289390764B

[49] M. F. Kadodwala, A. A. Davis, G. Scragg, B. C. C. Cowie, M. Kerkar, D. P. Woodruff, and R. G. Jones, *Surface Science*, vol. 324, p. 122, 1995. [Online]. Available: https://www.sciencedirect.com/science/article/pii/0039602894007152

[50] R. G. Jones, and M. Kadodwala, *Surface Science*, vol. 370, p. L219, 1997. [Online]. Available: https://www.sciencedirect.com/science/article/pii/S0039602896012988